EFFECTS OF SPATIALLY VARYING GROUND MOTIONS ON SHORT BRIDGES

By Thomas E. Price[1] and Marc O. Eberhard,[2] Members, ASCE

ABSTRACT: The effects of non-uniform excitation on short bridges were studied by computing the response of an idealized bridge to a suite of earthquake ground motions. The ground motions for each support were developed from seven measured ground motions and from idealizations of wave passage and coherency loss effects. For each set of support motions and for a range of bridge lengths and periods, the maximum support reactions were compared with the reactions calculated for coherent motions. For variable support motion, the contribution of the antisymmetric modes tended to increase, whereas the contribution of the symmetric modes generally decreased. Consequently, the dynamic component of the end support reaction computed using coherency loss excitation exceeded the response to coherent excitation for 62% of the bridges considered, varying from 75–180% of the coherent response. In contrast, the dynamic component of the central support reaction, which is affected only by symmetric modes, was unconservatively predicted in only 20% of the cases. Based on these observations, a method that relies on modifying the modal participation factor was developed for incorporating the effects of multisupport excitations into coherent response calculations.

INTRODUCTION

For many years, engineers have known that the spatial variation of strong ground shaking can significantly affect the response of long bridges (Abdel-Ghaffar and Rubin 1982; Dumanoglu and Severn 1990; Nazmy and Abdel-Ghaffar 1992). Since the advent of the SMART1 dense accelerograph array in Taiwan (Abrahamson 1985), it has been observed that this effect can be significant for shorter bridges as well (Harichandran and Wang 1988, 1990; Zerva, 1990, 1991). Most studies of the effects of spatially variable ground motion have been performed using random vibration methods that rely on an empirical characterization of the support motions, including power spectral density and coherency functions. Unfortunately, this implementation requires that some of the richness of measured earthquake accelerograms be neglected.

In this paper, an alternate analysis procedure is implemented. Recently, methods have been developed to generate directly earthquake acceleration histories consistent with recorded strong-motion array data (Hao et al. 1991; Abrahamson 1992, 1993) and empirical models of spatially coherency loss. For these ground motions, one can compute bridge response histories and response maxima directly. When computed for a number of bridge configurations and earthquake motions, these maxima can be used to determine circumstances in which the effects of spatially variable support excitation are significant. This procedure can also be used to develop design methods that account for spatially variable ground motion.

This study investigates the effects of multisupport excitation on the transverse response of a short bridge by evaluating response of an idealized bridge model to strong ground shaking from a suite of accelerograms. The bridge model, shown in Fig. 1, comprises a symmetric prismatic beam having two equal spans. Support motion time histories for a suite of accelerograms were generated corresponding to coherent, wave passage, and coherency loss models of spatially variable earthquake shaking. An empirical model of spatial coherency decay was enforced for the generated time histories using the procedure of Abrahamson (1992, 1993). Support reactions of the bridge were then computed via time history analysis. The change in response relative to coherent excitation was calculated for the wave passage and coherency loss excitations and for various combinations of bridge length and period. Finally, a modification to coherent response analysis is proposed to account for these effects.

[1]Asst. Prof., Mississippi State Univ., Box 9546, Mississippi State, MS 39762.

[2]Assoc. Prof., Univ. of Washington, Box 352700, Seattle, WA 98195.

Note. Associate Editor: Sashi K. Kunnath. Discussion open until January 1, 1999. To extend the closing date one month, a written request must be filed with the ASCE Manager of Journals. The manuscript for this paper was submitted for review and possible publication on October 16, 1997. This paper is part of the ***Journal of Structural Engineering***, Vol. 124, No. 8, August, 1998. ©ASCE, ISSN 0733-9445/98/0008-0948–0955/$8.00 + $.50 per page. Paper No. 16811.

MODEL OF SPATIALLY VARIABLE GROUND MOTION

Response of the idealized bridge model (Fig. 1) was computed for a suite of support acceleration time histories. Seven earthquake records, described in Table 1, were chosen to remove possible bias arising from the characteristics of an individual earthquake record. The time histories encompass a

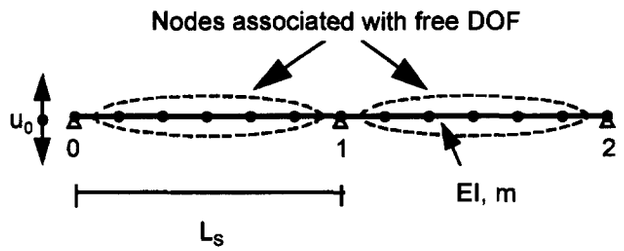

FIG. 1. Idealized Bridge Model

TABLE 1. Suite of Acceleration Time Histories

Earthquake (1)	Date (2)	Magnitude (3)	Focal mechanism (4)	Record (5)	Epicentral distance (6)	PGA (7)
El Centro	05/19/40	7.1	Strike-slip	Imperial Valley Irrigation District	9	342
Olympia	04/13/49	7.1	Interplate subduction	Olympia	30	161
Kern County	07/21/52	7.7	Reverse	Taft	43	173
Imperial Valley	10/15/79	6.8	Strike-slip	Differential Array Station 1	27	284
SMART1 Event 20 (Taiwan)	12/17/82	6.9	Reverse	Station I03	77	15
Coalinga	05/02/83	6.7	Reverse	Pleasant Valley Pump Plant, basement	9	267
Landers	06/28/92	7.3	Strike-slip	Lucerne Valley	2	735

Note: Magnitudes are M_S when available; M_L otherwise. Epicentral distances are in units of km. PGA are in units of cm/s^2.

variety of focal mechanisms, epicentral distances, and recording site conditions. Except for the SMART1 Event 20 record, the time histories are familiar to the engineering community and have been widely used in design practice. The SMART1 time history was included to provide a basis of comparison with the findings of Harichandran and Wang (1990).

Observed spatial variability in strong ground shaking is believed to arise from five sources: geometric attenuation, variation in local geology, wave passage effects, ray path effects, and extended source effects (Der Kiureghian 1996). Attenuation effects were not considered in this study, because they are only measurable over distances much larger than the short bridges considered. Local geology effects were not considered either, as they depend on a specific soil profile. The wave passage effect was used as a simple description of ground motion variability, because its implementation is straightforward and deterministic. Extended source and ray path effects were modeled as an ideal spatially varying stationary random process.

Spatially variable earthquake shaking measured at discrete locations is often described using the coherency function. For observations at two stations denoted by x and y, the frequency dependent coherency function can be written as

$$\gamma_{xy}(\omega) = \left[\frac{|S_{xy}|}{\sqrt{S_{xx}S_{yy}}}\right] \exp(i\vartheta_{xy}) \tag{1}$$

where S_{xy} = cross-spectral density, and S_{ss} and S_{yy} = power-spectral densities for observations x and y. Power- and cross-spectral densities are frequently estimated using smoothed periodograms computed from earthquake array records. The ϑ_{xy} term is a deterministic factor that accounts for wave passage between stations x and y and is a function of frequency, station separation distance, and apparent propagation velocity of the seismic disturbance

$$\vartheta_{xy} = \frac{\omega v}{V_{APP}} \tag{2}$$

where ω = circular frequency in rad/s; v = station separation distance; and V_{APP} = apparent propagation velocity of the disturbance. The apparent propagation velocity is itself a function of the characteristic velocity of the medium and the angle of incidence of the seismic disturbance.

The bracketed quantity in (1) is referred to as the lagged coherency, a real number between 0 and 1 that measures the fraction of energy that can be represented as a coherent wave traveling between the two locations. It is often assumed that this measure quantifies the effects of finite source dimension and ray path variability. In this study, the empirical model developed by Harichandran and Vanmarcke (1986) was used as a predictor of the lagged coherency. The authors modeled the lagged coherency as a weighted sum of exponential decay functions

$$|\gamma_{xy}(\omega, v)| = A \exp\left[\frac{-2v}{\alpha\theta}(1 - A + \alpha A)\right] + (1 - A)\exp\left[\frac{-2v}{\theta}(1 - A + \alpha A)\right] \tag{3}$$

where A and α are constants having values of 0.636 and 0.0186, respectively; and θ is a function of frequency having units of meters given by

$$\theta(\omega) = 31{,}200\left[1 + \left(\frac{\omega}{9.49}\right)^{2.95}\right]^{-1/2} \tag{4}$$

Note that the lagged coherency decreases with increasing frequency and station separation distance.

To provide a reasonable upper bound on the influence of the wave passage effect and to be consistent with studies by previous researchers (e.g., Harichandran and Wang 1990), an apparent propagation velocity of 1,000 m/s was used herein. This velocity is consistent with earthquake excitation composed primarily of surface waves, such as might be observed at an alluvial recording site located a moderate distance from the source. Similar values of V_{APP} were computed by O'Rourke and colleagues (O'Rourke et al. 1982; O'Rourke and El Hmadi 1988) using accelerograms from the 1971 San Fernando and 1979 Imperial Valley earthquakes.

GENERATION OF SPATIALLY VARIABLE GROUND MOTIONS

Using the procedure developed by Abrahamson (1992, 1993), three sets of support excitations were computed for each accelerogram listed in Table 1, corresponding to coherent, wave passage, and coherency loss excitation. In each case, the recorded accelerogram was taken as the ground motion at support 0, and motions were generated for supports 1 and 2. In the following, it is convenient to describe the support motions relative to support 0. If the amplitude and phase of the motion at support 0 is known (e.g., from a Fourier analysis of a recorded accelerogram), the amplitude and phase of the motion at the other supports are described using the relation

$$\mathbf{U}(\omega) = \Psi(\omega)U_0(\omega) \tag{5}$$

where $\mathbf{U}$ = a frequency-domain representation of the vector of support excitations; and U_0 = excitation at support 0. Ψ is a nondimensional spatial variability parameter that varies according to the ground motion model. This factor plays an important role in the dynamic response computations presented in this paper.

The first, and simplest, model of spatially variable support motions used was that of coherent excitation analysis, the current state of practice in the engineering community. Ψ is given in this case by the trivial equation

$$\Psi(\omega) = 1 \tag{6}$$

Next, the wave passage effect was used as a simple, deterministic model of spatially variable ground motion. The model assumes that an earthquake disturbance propagates as a coherent group of waves traveling at constant velocity, with the lagged coherency being implicitly set equal to unity. Using (1) and (2), the jth component of Ψ is given by

$$\Psi_j(\omega) = \exp\left(i\frac{\omega}{V_{APP}}jL_S\right) \tag{7}$$

where V_{APP} = apparent wave propagation velocity; and L_S = span length of the idealized bridge. A very large value of V_{APP} implies that the earthquake disturbance reaches each support simultaneously and is equivalent to the assumption of coherent excitation.

The third ground motion model included the loss of correlation among the support motions predicted by (3) and (4), as well as wave passage effects. Generating ground motions is more difficult in this case, because the lagged coherency defined in (1) must be satisfied between each pair of computed time histories. To compute time histories at n locations, it is necessary to satisfy the resulting $(n^2 - n)/2$ equations simultaneously for each frequency component of the acceleration time histories. Also, since the lagged coherency function is itself stochastic in nature, an element of randomness must be introduced into the computations.

For this study, the method developed by Abrahamson (1992, 1993) was used to generate the support acceleration and displacement time histories. This procedure requires that the Fourier amplitude spectrum of shaking at each support be set equal

to the spectrum at support 0. The model of coherency loss is then enforced by randomly perturbing the Fourier phase spectra of all stations from the value at support 0 and minimizing a penalty function based on (3) and (4). Wave passage effects are applied deterministically to the resulting time histories. Finally, the acceleration histories are baseline corrected to constrain the relative station displacements.

Because the Abrahamson procedure is probabilistic, it is not possible to write an expression for Ψ in closed form, as was done for the coherent and wave passage models. However, once suitable ground motions have been generated, it is possible to compute the components of Ψ on a frequency-by-frequency basis. To ensure consistency with (6) and (7), Ψ_j is given by

$$\Psi_j(\omega) = \frac{U_j(\omega)}{U_0(\omega)} \tag{8}$$

Support acceleration histories were computed for each combination of earthquake, model of spatially variable ground motion, and support separation distance. For several cases of coherency loss motion (four of the 35 generated support motions), the maximum displacement relative to support 0 occurred more than 10 s after the strong shaking portion of the record. Because this result seemed contradictory to the physics of the problem, these time histories were discarded and recomputed.

The strong shaking portion of example acceleration histories computed using the coherency loss model and a station separation distance of 30 m are shown in Fig. 2(a). While the acceleration records are similar, particularly in the longer period components, they vary in the higher frequencies consistently with the frequency-dependent model of coherency loss. Also, there is a delay equal to 0.03 s between adjacent supports, equal to the station separation distance divided by the apparent propagation velocity (1,000 m/s).

Figs. 2(b and c) show the lagged coherency computed for the example acceleration time histories. Because the lagged coherency is itself a biased estimator, the inverse hyperbolic tangent of lagged coherency is shown as the plot ordinate. Computed coherencies are shown as open circles, while the coherency model used to generate the time histories is shown as a solid line. Variation of the computed coherencies about the empirical model is consistent with the stochastic nature of the coherency function.

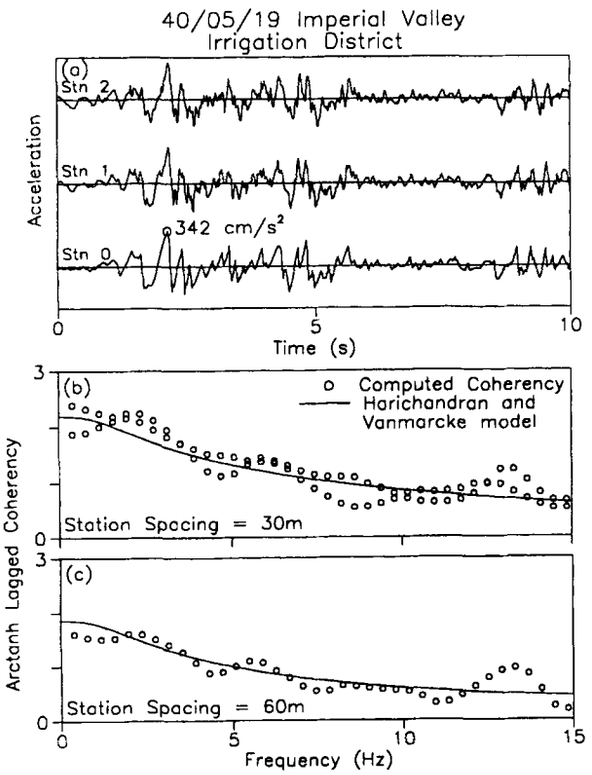

FIG. 2. Example Coherency Loss Support Acceleration Time Histories for L_s = 30 m: (a) Computed Time Histories; (b) and (c) Coherency Computed for Time Histories

SOLUTION OF EQUATIONS OF MOTION

Herein, the bridge was modeled as a two-span continuous beam with simply supported ends and uniform structural properties having n_F free degrees of freedom (DOF) and n_S support DOF (Fig. 1). The equations of motion for this system can be written as (Human 1990)

$$\begin{bmatrix} \mathbf{M}_{FF} & \mathbf{M}_{FS} \\ \mathbf{M}_{FSS}^T & \mathbf{M}_{SS} \end{bmatrix} \begin{bmatrix} \ddot{\mathbf{v}}_t \\ \ddot{\mathbf{u}} \end{bmatrix} + \begin{bmatrix} \mathbf{C}_{FF} & \mathbf{C}_{FS} \\ \mathbf{C}_{FS}^T & \mathbf{C}_{SS} \end{bmatrix} \begin{bmatrix} \dot{\mathbf{v}}_t \\ \dot{\mathbf{u}} \end{bmatrix} + \begin{bmatrix} \mathbf{K}_{FF} & \mathbf{K}_{FS} \\ \mathbf{K}_{FS}^T & \mathbf{K}_{SS} \end{bmatrix} \begin{bmatrix} \mathbf{v}_t \\ \mathbf{u} \end{bmatrix} = \begin{bmatrix} \mathbf{0} \\ \mathbf{f}_S \end{bmatrix} \tag{9}$$

where $\mathbf{M}$, $\mathbf{C}$, and $\mathbf{K}$ = structural property matrices, partitioned into free DOF ($*_{FF}$) and support DOF ($*_{SS}$). The model DOF have been also partitioned into free DOF ($\mathbf{v}_t$) and support DOF ($\mathbf{u}$). The reaction forces at the supports are given by $\mathbf{f}_S$.

One can solve (9) for the active DOF by describing $\mathbf{v}_t$ as the sum of two components, known as the pseudostatic response ($\mathbf{v}_{st}$) and the dynamic response ($\mathbf{v}_d$). The pseudostatic response results from the differential support displacements in the absence of inertial loading. Neglecting the inertial loading terms, the pseudostatic response can be computed using

$$\mathbf{v}_{st} = -\mathbf{K}_{FF}^{-1}\mathbf{K}_{FS}\mathbf{u} \tag{10}$$

The multiplier of the support motions, $-\mathbf{K}_{FF}^{-1}\mathbf{K}_{FS}$, is a matrix of dimension n_F by n_S, wherein the kth column represents the deflected shape of the structure resulting from a unit displacement applied at the kth support.

The dynamic response ($\mathbf{v}_d$) is caused by inertial loading of the structure. It can be computed by multiplying out the first row of (9), eliminating $\mathbf{v}_{st}$ using (10), and neglecting loading due to damping effects. In the case of a lumped mass matrix, the final equation for $\mathbf{v}_d$ is given by

$$\mathbf{M}_{FF}\ddot{\mathbf{v}}_d + \mathbf{C}_{FF}\dot{\mathbf{v}}_d + \mathbf{K}_{FF}\mathbf{v}_d = \mathbf{M}_{FF}\mathbf{K}_{FF}^{-1}\mathbf{K}_{FS}\ddot{\mathbf{u}} \tag{11}$$

If the mass and stiffness matrices possess normal modes and the damping matrix is orthogonal, an expression for the jth modal ordinate can be written as

$$\ddot{y}_j + 2\omega_j\xi_j\dot{y}_j + \omega_j^2 y_j = \phi_j^T\mathbf{M}_{FF}\mathbf{K}_{FF}^{-1}\mathbf{K}_{FS}\ddot{\mathbf{u}} \tag{12}$$

where y_j = jth modal ordinate; ϕ_j = mass-normalized mode shape of the jth mode; and ω_j and ξ_j = natural circular frequency and damping ratio of mode j, respectively.

A frequency domain solution was used to solve (12). For a case in which the support motion is a complex harmonic motion of frequency ω whose amplitude is given by (5) the equation of the jth modal coordinate is found by substituting (5) into (12) as follows:

$$\ddot{Y}_j + 2\omega_j\xi_j\dot{Y}_j + \omega_j^2 Y_j = (\phi_j^T\mathbf{M}_{FF}\mathbf{K}_{FF}^{-1}\mathbf{K}_{FS})(-\omega^2\Psi(\omega)U_0(\omega)e^{-i\omega t}) \tag{13}$$

where Y_j = Fourier component of y_j corresponding to frequency ω.

A harmonic solution for Y_j can be obtained by solving the linear differential equation

$$Y_j = A_j B_j U_0(\omega)e^{-i\omega t} \tag{14}$$

where A_j = familiar dynamic amplification factor (e.g., Humar

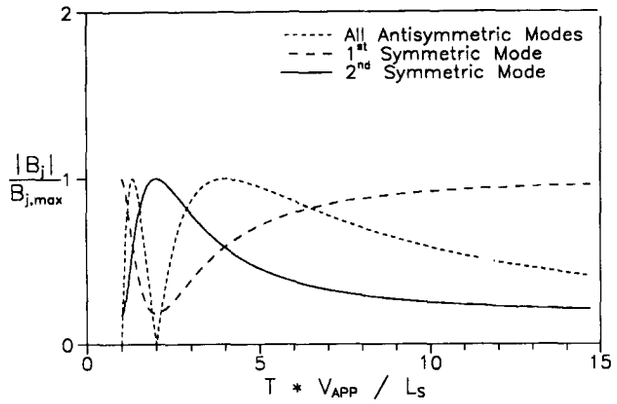

FIG. 3. Generalized Participation Factor for Selected Modes of Continuous Two-Span Beam

1990); and B_j = frequency-dependent generalized participation factor for mode j given by

$$B_j = (\phi_j^T \mathbf{M}_{FF} \mathbf{K}_{FF}^{-1} \mathbf{K}_{FS}) \Psi(\omega) \tag{15}$$

B_j is a complex scalar function of only the structural geometry and the model of ground motion spatial variability. For coherent input motion, B_j is equal to the coherent participation factor.

As B_j is independent of the properties of the support time histories, (15) can be used to predict the influence of spatially variable excitation on structural response. Fig. 3 shows the magnitude of the generalized participation factor (B_j) for the first few modes of the idealized bridge, evaluated using the wave passage ground motion model given in (7). The nondimensional period TV_{APP}/L_S is used as the abscissa of Fig. 3, where $T = 2\pi/\omega$, and $|B_j|$ has been normalized by its limiting value, which is given by

$$B_{j,\max} = \sum_i |(\phi_j^T \mathbf{M}_{FF} \mathbf{K}_{FF}^{-1} \mathbf{K}_{FS})_i| \tag{16}$$

For each mode, $|B_j|$ approaches the coherent value in the limit as $TV_{APP}/L_S \to \infty$. Eq. (15) yields the same curve for all antisymmetric modes of the two-span beam considered in this study, which increases from its coherent value (0) to peaks at TV_{APP}/L_S = 4, 4/3, ... For wave passage excitation, the response of symmetric modes either increases or decreases, depending on the mode. The response of the first symmetric mode decreases for finite apparent propagation velocities while the second symmetric modal response increases. A depiction such as Fig. 3 can be used to predict whether the effects of wave passage excitation will increase or decrease a particular response quantity, depending on the contribution of the various modes to that quantity.

Using the solution for simple harmonic excitation given in (14) and (15) and techniques of Fourier synthesis, the modal coordinates y_j can be computed for each set of support motions used in this study. The dynamic displacement response is then recovered using modal superposition, and total response is obtained by adding the dynamic response and the pseudostatic response computed from (10). Finally, support reactions can be computed using the second row of (9).

PROPERTIES OF BRIDGE MODELS

The properties of the two-span bridge model must be specified to apply the aforementioned solution procedure. To ensure that the bridge model would have typical properties, bridge lengths and fundamental lateral periods were chosen using the ambient vibration database of Dusseau and Dubaisi (1993). The measured lengths and periods of short-span

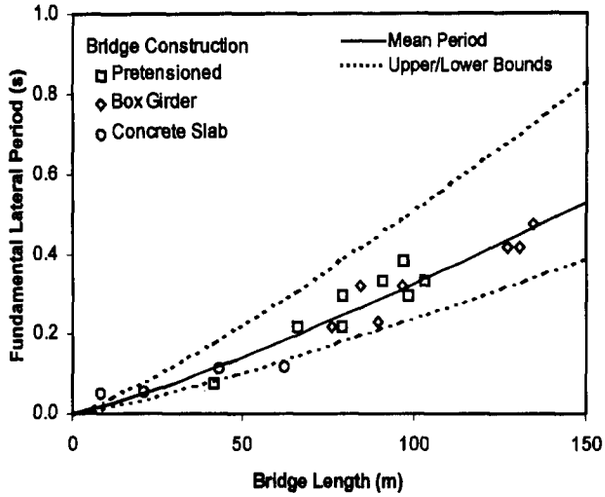

FIG. 4. Fundamental Lateral Periods of Short Bridges (Dusseau and Dubaisi 1993)

bridges are plotted in Fig. 4 for several types of bridge construction. The data for all bridge types were used to develop a relation between bridge length and fundamental lateral period having the form

$$T_0 = \frac{L^n}{a} \tag{17}$$

where T_0 = fundamental lateral bridge period in seconds; L = total bridge length in meters; and a and n = calibration constants. Nonlinear regression was used to determine the best-fit curve for the database, plotted as the solid line in Fig. 4 (a = 780, n = 1.20).

The regression data were then used to compute a 90% lognormal confidence interval about the best fit. The lower bound of this interval (a = 1,060) was selected as the lower bound for bridge periods. Based on the recommendations of *ATC-32* ("Improved" 1996), it was assumed that the effective *EI* under strong ground shaking would be reduced by 25% from the ambient vibration value. Therefore, the upper bound of the confidence interval was increased by an additional 15%, resulting in a final upper bound "a" value of 480. Upper and lower bounds are shown as the dashed curves in Fig. 4. These bounds agree well with the results of Mahmoodzadegan et al. (1994), who measured a transverse period of 0.07 s for a 30 m long bridge subjected to quick-release vibration. They agree also with the fundamental period of the 63 m long Meloland Road Overcrossing measured during quick-release testing (0.30 s) (Werner et al. 1990).

Span lengths of 10, 20, 30, 40, and 60 m were chosen to represent the bridges in the database, assuming a bridge composed of two equal spans. A range of fundamental periods between the computed upper and lower bounds was used in the response computations.

Modal periods and frequencies for higher modes of the idealized bridge were computed using the fact that the modal frequencies have fixed ratios based on the bridge geometry. By static condensation of the beam rotational degrees of freedom, the mass and stiffness matrices of the idealized bridge can be written as

$$\mathbf{M}_{FF} = mL_S \bar{\mathbf{M}}_{FF}; \quad \mathbf{K}_{FF} = \frac{EI}{L_S^3} \bar{\mathbf{K}}_{FF} \tag{18}$$

where EI = flexural rigidity of the beam; m = mass per unit length; and L_S = span length. The quantities denoted with an overbar are nondimensional and depend only on the bridge geometry. Lumped-mass and standard beam stiffness formu-

lations were used in the structural property matrices, which were generated from a finite element model having 49 total degrees of freedom.

Normal modes of the structure are computed using the eigenvalue equation given by

$$(\mathbf{K}_{FF} - \omega_j^2 \mathbf{M}_{FF})\phi_j = \mathbf{0} \tag{19}$$

Substituting (18) into (19) and dividing through by EI/L_S^3, the eigenvalue equation is given by

$$\left(\bar{\mathbf{K}}_{FF} = \omega_j^2 \frac{mL_S^4}{EI} \bar{\mathbf{M}}_{FF}\right) \phi_j = \mathbf{0} \tag{20}$$

It can be seen by inspection of (20) that the mode shapes of the structure are independent of the structural properties of the beam (EI, m, and L_S) and depend only on the boundary conditions. Also, the modal frequencies are now given in nondimensional form, implying that it is not necessary to specify the structural properties directly in order to model the beam. Natural frequencies for modes other than the first can then be computed using the ratios of the nondimensional frequencies. In the interest of limiting computational cost, only the first 28 modes of the bridge, corresponding to over 99% of the participating mass, were used in the response computations.

COMPUTED DYNAMIC RESPONSE

Time history analyses were performed for 1,638 combinations of bridge length, fundamental period, ground motion model, and earthquake accelerogram to compute the maximum dynamic response amplitude ($\mathbf{v}_d$). The greater maximum absolute support reaction at supports 0 and 2 was reported as the maximum end support reaction for the structure. Because observed seismic bridge damage (Hall 1995) indicates that support elastic force demand is a critical design concern, particularly in brittle structures, this paper presents computed support reactions only. Price and Eberhard (1996) report additional response quantities, including relative midspan displacements, bending moments, and the sum of support reactions.

To facilitate comparison of the maximum response computed for coherent excitation with that computed for noncoherent motions, the maximum wave passage and coherency loss dynamic responses were normalized by the maximum coherent response. A ratio greater than 1.0 indicates that coherent response analysis was unconservative. Normalized dynamic response ratios for end support reaction and central support reaction are plotted against the dimensionless parameter $T_0 V_{APP}/L_S$ in Fig. 5. This parameter is equivalent to the ratio of the fundamental structural period to the time a seismic disturbance takes to traverse a span of the bridge. Use of this

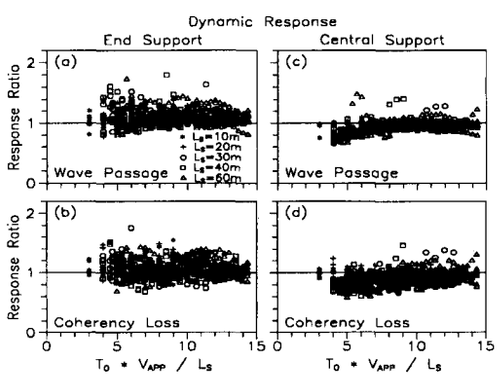

FIG. 5. Ratios of Dynamic Wave Passage and Coherency Loss Support Reaction to Coherent Support Reaction: (a) and (b) End Support; (c) and (d) Central Support

TABLE 2. 90% Upper-Brand Dynamic Response Ratios

Response quantity (1)	Normalized by Coherent Response: Wave passage (2)	Normalized by Coherent Response: Coherency loss (3)	Normalized by Approximate Response: Wave passage (4)	Normalized by Approximate Response: Coherency loss (5)
End support reaction	1.28	1.27	1.03	1.04
Central support reaction	1.07	1.07	0.94	0.97
Midspan displacement[a]	1.57	1.58	1.08	1.10
Central support moment[a]	1.02	1.03	0.96	0.98
Sum of support reactions[a]	0.98	1.00	0.96	0.99

Note: Upper bounds correspond to a 90% one-sided Gaussian confidence interval. Midspan displacement measured relative to a chord through the end supports.

[a]Data reported in Price and Eberhard (1996).

parameter removes the influence of the value of V_{APP} from the wave passage response computations. Since V_{APP} was chosen to represent a lower bound in this study, the influence of wave passage effects may be taken as an upper bound, relative to coherency loss.

The end support reaction response ratios shown in Figs. 5(a and b) indicate that coherent response analysis was unconservative in most cases. Response ratios greater than 1 were computed over the entire range of $T_0 V_{APP}/L_S$ for both wave passage and coherency loss excitations. The maximum wave passage end support reaction was underpredicted by coherent analysis for 77% of the computations, by an average of 10%. Similarly, coherency loss response was underpredicted by coherent analysis for 62% of the analyses and by an average of 7%. Most importantly, several response ratios greater than 1.5 were computed. Table 2 reports statistical 90% upper bounds for the response ratios for various response quantities. For end support reactions, the 90% upper bound response ratios were 1.28 for wave passage excitation and 1.27 for coherency loss excitation.

In contrast, central support reaction response ratios were generally less than 1 [Figs. 5(c and d)]. Coherent analyses were unconservative for wave passage and coherency loss excitation in less than 20% of the cases. Coherent analysis was conservative by an average of 14% for wave passage excitation and 17% for coherency loss excitation. Central support reaction 90% upper-bound response ratios were 1.07 for both wave passage and coherency loss excitation.

It is significant that the effects of variable support excitation differ for the end and central support reactions. The difference is attributable to the fact that the contributing modes for each response quantity are affected differently by multisupport excitation effects, as discussed previously. The central support reaction is dominated by the contribution of the first symmetric mode, which exhibits reduced participation under wave passage excitation, as shown in Fig. 3. On the other hand, the end support reaction receives a significant contribution from the antisymmetric modes, for which response is increased by wave passage effects, also shown in Fig. 3. The 90% upper-bound dynamic response ratios in Table 2 indicate that similar phenomena were observed for relative midspan displacement (antisymmetric modes contribute significantly), and central support moment (dominated by first symmetric mode), and the sum of support reactions (dominated by first symmetric mode).

One might expect that bridge length would have a strong influence on the response to variable support excitation. Sta-

tistical analysis of the data plotted in Fig. 5 indicates, however, that the dependence of dynamic response ratio on bridge length is not significant. Observed differences are small relative to the overall variability of the data.

COMPUTED TOTAL RESPONSE

Ratios of maximum wave passage and coherency loss response to maximum coherent response were also computed for total response, which is the sum of the dynamic and pseudostatic components. Total response ratios for end support reaction and central support reaction are shown in Fig. 6. Response ratios that would appear outside the plotted area are denoted by an arrow indicating a larger value.

The relative influence of the pseudostatic and dynamic response components can be seen by comparing Figs. 5 and 6. The contribution of pseudostatic response does not significantly affect wave passage response for either reaction; total response ratios are similar to dynamic response ratios in both cases. Coherency loss response, however, has a significant pseudostatic component, especially at small values of T_0V_{APP}/L_S and shorter span bridges. For values of T_0V_{APP}/L_S less than approximately 8 and span lengths less than or equal to 20 m, many total response ratios greater than 2 were computed.

To compare the magnitude of the computed coherency loss pseudostatic response maxima with the results of other researchers, the maximum deflection of the central support relative to a chord through the end supports was computed for each set of support time histories. Maximum pseudostatic deformations and stresses of the idealized bridge can be shown to be proportional to this quantity. The computed maximum deflections were roughly equal to $0.08L_Su_{max}$, where u_{max} = maximum displacement at support 0, and L_S is given in meters. Although this value corresponds to a pseudostatic response greater than that predicted by other researchers (Harichandran and Wang 1990; Der Kiureghian (1991), analysis of accelerograms recorded at the Chiba array (Katayama et al. 1990) indicates that even larger pseudostatic response may occur. Furthermore, computations presented by Zerva (1992) demonstrate that the relative displacements are highly sensitive to the choice of coherency model. Clearly, direct field measurements of spatially varying displacement caused by earthquake shaking are needed to refine estimates of pseudostatic response.

Response of a two-span beam to spatially variable excitation has been studied by Harichandran and Wang (1990) and Zerva (1990, 1991) using random vibration methodology and by Der Kiureghian and Neuenhofer (1991) using response spectrum analysis. Harichandran and Wang (1990) and Der Kiureghian and Neuenhofer (1991) present computations for moment over the central support that indicates this quantity is reduced for non-uniform excitation. These findings are consistent with the 90% inner bound central support moment response ratios computed in this study (Table 2).

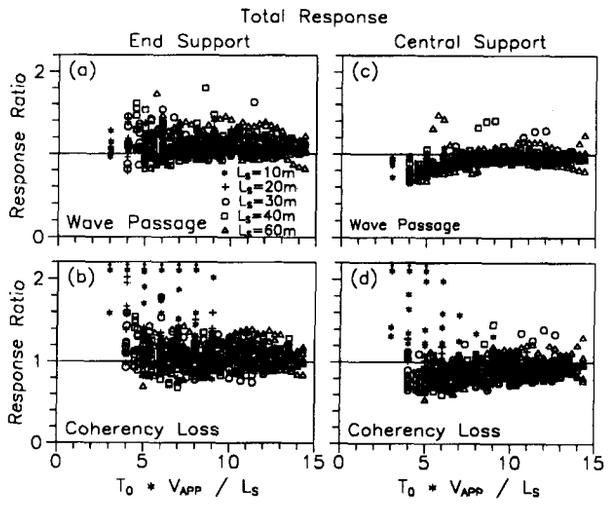

FIG. 6. Ratios of Total Wave Passage and Coherency Loss Support Reaction to Coherent Support Reaction: (a) and (b) End Support; (c) and (d) Central Support

The maximum absolute midspan displacement was decreased by spatially variable excitation, as found by the previous researchers. This response quantity, however, is strongly influenced by the presence of a rigid-body component of bridge response. When the rigid-body motion was removed from the midspan displacement computations, relative midspan displacement increased significantly over coherent response (Table 2). Because both relative midspan displacement and end support reaction are nonzero in the antisymmetric modes, this finding is consistent with the end support reaction response ratios in Figs. 5 and 6. The trend in the computed reactions agree with Zerva (1990, 1991), who found that bridges subjected to wave passage excitation could experience increased end support reactions over a range of apparent propagation velocities, for certain combinations of bridge length and period.

APPROXIMATE DYNAMIC RESPONSE COMPUTATION

Methods have been proposed previously to account for the effects of support excitation (Abrahamson 1985; Yamamura and Tanaka 1990; Der Kiureghian and Neuenhofer 1991; Berrah and Kausel 1992). In general, these methods either require a prohibitive number of numerical integrations, or cannot be extended to structures with modes having a vanishing coherent participation factor.

The method presented in this paper was developed based on the observation both herein (Fig. 5, Table 2) and in previous studies (e.g., Zerva 1990) that a loss of coherency generally leads to a reduced response. It should be possible, therefore, to conservatively estimate maximum response using wave passage excitation alone. Luco and Wong (1986) reached a similar conclusion for the analysis of a rigid foundation, wherein response to partially coherent excitation was conservatively predicted using properly calibrated wave passage analysis. This approach is attractive because the wave passage model is deterministic, admits closed-form solution, and is less computationally expensive to implement than the coherency loss model. Furthermore, the proposed method can be applied to any analysis in which spatially variable ground shaking can be described deterministically (e.g., using site response analysis).

The approximation was implemented by modifying the participation factor used in coherent analysis to account for the influence of wave passage effects. The generalized modal participation factor defined in (15) and plotted in Fig. 3 yields a frequency-dependent measure of the interaction between a given mode of the structure and the effects of wave passage support excitation. If the mode being excited is lightly damped, then the excitation is filtered sharply about the mode's natural frequency. It is proposed to neglect the frequency dependence of B_j and set the participation factor equal to the magnitude of B_j evaluated at the natural frequency of the mode. To ensure a conservative approximation, the value of $|B_j|$ used herein was not allowed to be less than the coherent participation factor. Using this substitution, analysis can be carried out as for coherent analysis, with the only exception being the definition of the participation factor.

It should be noted that the curves shown in Fig. 3 are appropriate only for the bridges considered in this study and that T_j, V_{APP}, and L_S must be specified to evaluate $|B_j|$. However,

it would be computationally inexpensive to use a representation such as Fig. 3 to choose a conservative value of $|B_j|$ for other structures. The potential effects of variability in T_j, V_{APP}, and L_S can also be evaluated in this manner.

Approximate response was computed for each of the bridges analyzed previously and for each of the time histories in the suite of accelerograms. Modal response time histories were computed by multiplying time histories from appropriate single-degree-of-freedom response time histories with the modified participation factors. Approximate dynamic response was then computed using modal superposition. Finally, the computed dynamic wave passage and coherency loss response were normalized with respect to the approximate response. The resulting end and central support reaction response ratios are plotted in Fig. 7.

End support reactions to wave passage excitation were conservatively estimated for 86% of the analyses, while coherency loss response was conservatively estimated for 83% of the analyses. 90% upper-bound response ratios computed using approximate responses are shown in Table 2. Although the approximated values are conservative overall, predictions are unconservative by as much as 20% for seven of the 1,092 computed quantities. For central support reactions, the approximate analyses were conservative for 100% of the wave passage cases and 95% of the coherency loss cases.

Comparison of the coherent and approximate response 90% upper bounds (Table 2) shows that the approximate analyses provide a rational, improved estimate of the effects of spatially variable excitation. Each of the response quantities is conservatively predicted, without adding unnecessary conservatism to the computations. The method was also found to work well when applied to the relative midspan displacement, the central support moment, and the sum of the support reactions (Table 2). Furthermore, the approximate method can be implemented using commonly available software that assumes uniform support motions. The approximation also leads to tremendous savings over coherency loss analysis, because it is unnecessary to perform the costly generation of support acceleration histories needed for each combination of ground motion and span length.

The proposed method provides a greatly improved estimate of maximum dynamic response compared with coherent response analysis. For cases in which differential support displacements dominate total response, an estimate of pseudostatic response must be included in the analysis. Unfortunately, direct measurements of earthquake-induced differential displacements are insufficient to justify such an estimate at this time.

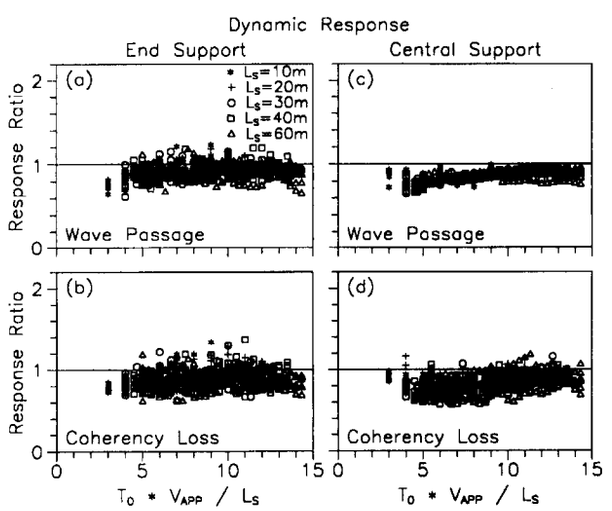

FIG. 7. Ratios of Computed Wave Passage and Coherency Loss Support Reaction to Approximate Support Reaction: (a) and (b) End Support; (c) and (d) Central Support

SUMMARY

Computations were performed to determine the effects of spatially variable ground motion on the response of short bridges. Sets of support acceleration time histories were generated using a suite of accelerograms (Table 1) in conjunction with coherent, wave passage, and coherency loss models of spatially variable ground motion. Bridge support reaction time histories were computed for each excitation. Response to spatially variable support excitation was then compared with coherent response. Parametric studies were performed to determine the importance of bridge period and length in response to multisupport excitation. The findings of the study can be summarized as follows:

1. The dynamic response of short bridges can be influenced significantly by the effects of variable support excitation. For most of the bridges considered in this study, coherent analysis provided a conservative estimate of the dynamic central support reaction, the central support moment, and the sum of support reactions of the idealized two-span bridge. However, end support reactions and relative midspan displacements were consistently underpredicted by coherent response analysis. The average error was only 10%, but for many combinations of bridge length, bridge period, and earthquake excitation, coherent analysis was unconservative in some cases by as much as 50%.
2. Spatially variable excitation affects each response quantity differently depending on the contribution of individual modes. For each response quantity considered, the influence of spatially variable excitation was consistent with the generalized participation factor of the dominant mode for the response quantity (Fig. 3). For example, the antisymmetric modes contributed significantly to the end support reaction; as a result, response to multisupport excitation significantly exceeded the response to coherent excitation. The central support reaction, however, was strongly influenced by the first symmetric mode, so it decreased when spatial variability was taken into account. Similar behavior was observed for relative midspan displacement, central support moment, and the sum of support reactions. These trends with respect to increased/decreased modal contribution are observed for both wave passage and coherency loss models of spatially variable ground motion.
3. For the coherency loss model implemented in this study, the bridges studied can be divided into two categories, based on whether the pseudostatic or dynamic response dominated the total response. Bridges for which T_0V_{APP}/L_S was small were found to have strong components of pseudostatic response when subjected to coherency loss excitation. Response of bridges with large values of T_0V_{APP}/L_S was dominated by the dynamic component of response. The value of T_0V_{APP}/L_S at which this change was observed depended on the relative support displacements, for which few corroborative field measurements are available, and on the properties of the structural model.
4. The dynamic response of short bridges excited by the wave passage and coherency loss models can be conservatively approximated by modifying the modal participation factor to include the effects of wave passage excitation. The proposed method is attractive because it can easily be extended to structures other than those considered, it can be used with any deterministic description of spatially variable ground motion, and it is computation-

ally inexpensive. The method can be easily automated and used in conjunction with currently available finite element analysis software.

APPENDIX I. REFERENCES

Abdel-Ghaffar, A. M., and Rubin, L. I. (1982). "Suspension bridge response to multiple-support excitations." *J. Engrg. Mech. Div.*, ASCE, 108(2), 419–435.

Abrahamson, N. A. (1985). "Estimation of seismic wave coherency and rupture velocity using the SMART1 strong-motion array recordings." *Rep. UCB/EERC-85/02*. Earthquake Engineering Research Center, University of California, Berkeley, Calif.

Abrahamson, N. A. (1992). "Generation of spatially incoherent strong motion time histories." *Proc., 10th World Conf. on Earthquake Engrg.*, A. A. Balkema, Rotterdam, The Netherlands, 10, 845–850.

Abrahamson, N. A. (1993). "Spatial variation of multiple support inputs." *Proc., 1st U.S. Seminar, Seismic Evaluation and Retrofit of Steel Bridges*, University of California, Berkeley, Calif.

Berrah, M., and Kausel, E. (1992). "Response spectrum analysis of structures subjected to spatially varying motions." *Earthquake Engrg. and Struct. Dynamics*, 21, 461–470.

Der Kiureghian, A. (1996). "A coherency model for spatially varying ground motions." *Earthquake Engrg. and Struct. Dynamics*, 25, 99–111.

Der Kiureghian, A., and Neuenhofer, A. (1991). "A response spectrum method for multiple-support seismic excitations." *Rep. UCB/EERC-91/08*. Earthquake Engineering Research Center, University of California, Berkeley, Calif.

Dumanoglu, A. A., and Severn, R. T. (1990). "Stochastic response of suspension bridges to earthquake forces." *Earthquake Engrg. and Struct. Dynamics*, 19, 135–152.

Dusseau, R. A., and Dubaisi, H. N. (1993). "Natural frequencies of concrete bridges in the Pacific Northwest." *Transp. Res. Rec. 1393*, Transportation Research Board, Washington, D.C., 119–132.

Hall, J. H. (ed.). (1995). "Northridge earthquake reconnaissance report. Volume 1." *Earthquake Spectra*, Earthquake Engineering Research Institute, Oakland, Calif., 11 (Supplement C), 515–523.

Hao, H., Oliviera, C. S., and Penzien, J. (1991). "Multiple-station ground motion processing and simulation based on SMART1 array data." *Nuclear Engrg. and Design*, 111, 293–310.

Harichandran, R. S. (1991). "Estimating the spatial variation of earthquake ground motions from dense array recordings." *Struct. Safety*, Amsterdam, The Netherlands, 10, 219–233.

Harichandran, R. S., and Vanmarcke, E. H. (1986). "Stochastic variation of earthquake ground motion in space and time." *J. Engrg. Mech.*, ASCE, 112(2), 154–174.

Harichandran, R. S., and Wang, W. (1988). "Response of simple beam to spatially varying earthquake excitation." *J. Engrg. Mech.*, ASCE, 114(9), 1526–1541.

Harichandran, R. S., and Wang, W. (1990). "Response of indeterminate two-span beam to spatially varying seismic excitation." *Earthquake Engrg. and Struct. Dynamics*, 19, 173–187.

Humar, J. L. (1990). *Dynamics of structures*. Prentice Hall, Inc., Englewood Cliffs, N.J.

"Improved seismic design criteria for California bridges: provisional recommendations." (1996). *Rep. ATC-32*, Applied Technology Council, Redwood City, Calif.

Katayama, T., Yamazaki, F., Nagata, S., Lu, L., and Türker, T. (1990). "Development of strong motion database for the Chiba Seismometer Array." *Rep. 90-1(14)*. Earthquake Disaster Mitigation Engineering, Institute of Industrial Science, University of Tokyo, Tokyo, Japan.

Luco, J. E., and Wong, H. L. (1986). "Response of a rigid foundation to a spatially random ground motion." *Earthquake Engrg. and Struct. Dynamics*, 14, 891–908.

Mahmoodzadegan, B., Mander, J. B., and Chen, S. S. (1994). "Simplified seismic evaluation for a class of slab-on-girder bridge." *Proc., 5th U.S. National Conf. on Earthquake Engrg.*, Earthquake Engrg. Res. Inst., Oakland, Calif., 1, 521–530.

Nazmy, A. S., and Abdel-Ghaffar, A. M. (1992). "Effects of ground motion spatial variability on the response of cable-stayed bridges." *Earthquake Engrg. and Struct. Dynamics*, 21, 1–20.

O'Rourke, M. J., Bloom, M. C., and Dobry, R. (1982). "Apparent propagation velocity of body waves." *Earthquake Engrg. and Struct. Dynamics*, 10, 283–294.

O'Rourke, M. J., and El Hmadi, K. (1988). "Analysis of continuous buried pipelines for seismic wave effects." *Earthquake Engrg. and Struct. Dynamics*, 16, 917–929.

Price, T. E., and Eberhard, M. O. (1996). "Response history analyses of short bridges subjected to spatially-varying ground motion." *SGEM Rep. No. 96-3*. Department of Civil Engineering, University of Washington, Seattle, Wash.

Spudich, P. (1994). "Recent seismological insights into the spatial variation of earthquake ground motions." *New developments in earthquake ground motion estimation and implications for engineering design practice*. Applied Technology Council, Redwood City, Calif., 13.1–13.31.

Werner, S. D., Beck, J. L., and Nisar, A. (1990). "Dynamic tests and seismic excitation of a bridge structure." *Proc., 4th U.S. National Conf. on Earthquake Engrg.*, 1, 1037–1046.

Yamamura, N., and Tanaka, H. (1990). "Response analysis of flexible MDF systems for multiple-support seismic excitations." *Earthquake Engrg. and Struct. Dynamics*, 19, 345–357.

Zerva, A. (1990). "Response of multi-span beams to spatially incoherent seismic ground motions." *Earthquake Engrg. and Struct. Dynamics*, 19, 819–832.

Zerva, A. (1991). "Effect of spatial variability and propagation of seismic ground motions on the response of multiply supported structures." *Probabilistic Engrg. Mech.*, Essex, U.K. 6, 212–221.

Zerva, A. (1992). "Seismic loads predicted by spatial variability models." *Struct. Safety*, Amsterdam, The Netherlands, 11, 227–243.

APPENDIX II. NOTATION

The following symbols are used in this paper:

A = dynamic amplification factor;
A, α = constants for empirical model of coherency decay;
a, n = regression coefficients for bridge period database;
B = generalized modal participation factor;
EI, m = flexural rigidity and mass per unit length of idealized bridge model;
$\mathbf{f}_r$ = support reactions;
L, L_S = total length and span length of bridge;
$\mathbf{M}$, $\mathbf{C}$, $\mathbf{K}$ = mass, damping, and stiffness matrices of idealized bridge model;
S_{xy} = cross-spectral density between signals observed at stations x and y;
T_0 = fundamental bridge period;
$\mathbf{u}$, $\mathbf{U}$ = time- and frequency-domain values of support motion;
V_{APP} = apparent propagation velocity of seismic disturbance;
$\mathbf{v}_t$, $\mathbf{v}_{st}$, $\mathbf{v}_d$ = total, pseudostatic, and dynamic response components for model degrees of freedom;
y, Y = time- and frequency-domain values of jth modal response history;
γ_{xy} = coherency between signals measured at locations x and y;
ϑ_{xy} = phase term of coherency loss;
ν = station separation distance;
Ψ = spatial variability of earthquake ground motion;
ω = circular natural frequency (rad/s); and
ω, ξ, ϕ = frequency, damping ratio, and shape of mode j.

Subscripts

i = support or station number; and
j = mode number.